HHS Public Access

Author manuscript

Clin Cancer Res. Author manuscript; available in PMC 2021 April 01.

Published in final edited form as:

Clin Cancer Res. 2020 October 01; 26(19): 5129–5139. doi:10.1158/1078-0432.CCR-20-1025.

A Phase 2 Study of Allogeneic GM-CSF Transfected Pancreatic Tumor Vaccine (GVAX) with Ipilimumab as Maintenance Treatment for Metastatic Pancreatic Cancer

Annie A. Wu[1,*], **Katherine M. Bever**[1,*], **Won Jin Ho**[1], **Elana J. Fertig**[1], **Nan Niu**[1,2], **Lei Zheng**[1], **Rose M. Parkinson**[1], **Jennifer N. Durham**[1], **Beth Onners**[1], **Anna K. Ferguson**[1], **Cara Wilt**[1], **Andrew H. Ko**[3], **Andrea Wang-Gillam**[4], **Daniel A. Laheru**[1], **Robert A. Anders**[1,5], **Elizabeth D. Thompson**[1,5], **Elizabeth A. Sugar**[1,6], **Elizabeth M. Jaffee**[1], **Dung T. Le**[1]

[1]Department of Oncology, Sidney Kimmel Comprehensive Cancer Center, The Skip Viragh Center for Pancreas Cancer Clinical Research and Patient Care, and The Bloomberg-Kimmel Institute for Cancer Immunotherapy at Johns Hopkins University School of Medicine, Baltimore, MD, USA

[2]Department of Gastrointestinal and Pancreatic Surgery, Zhejiang Provincial People's Hospital, Hangzhou, Zhejiang 310014, China

[3]Department of Medicine, Division of Hematology/Oncology, UCSF Helen Diller Family Comprehensive Cancer Center at University of California, San Francisco, CA, USA

[4]Department of Internal Medicine, Division of Oncology at Washington University School of Medicine, St. Louis, MO, USA

[5]Department of Pathology, Johns Hopkins University School of Medicine, Baltimore, MD, USA

[6]Department of Biostatistics, Johns Hopkins University Bloomberg School of Public Health, Baltimore, MD, USA

Abstract

Purpose: This phase 2 study tested granulocyte-macrophage colony-stimulating factor-secreting allogeneic pancreatic tumor cells (GVAX) and ipilimumab in metastatic pancreatic ductal adenocarcinoma (PDA) in the maintenance setting.

Methods: Patients with PDA who were treated with front-line chemotherapy consisting of 5-fluorouracil, leucovorin, irinotecan, and oxaliplatin (FOLFIRINOX) in the metastatic setting and had ongoing response or stable disease after 8–12 doses were eligible. Patients were randomized 1:1 to treatment with GVAX and ipilimumab given every 3 weeks for 4 doses then every 8 weeks

Corresponding Author: Dung T. Le, M.D., 1650 Orleans St, CRB1 410, Baltimore, MD 21287, Phone: 443-287-0002, dle@jhmi.edu.

*Contributed equally

Conflicts of Interest

D.T.L. is a paid consultant for Bristol Myers Squibb and receives research funding. E.M.J has the potential to accept royalties for a patent from Aduro BioTech Inc. All of the remaining authors have no financial conflicts of interest related to the publication of this work.

Clinical trial information: NCT01896869

(Arm A) or to FOLFIRINOX continuation (Arm B). The primary objective was to compare overall survival (OS) between the two arms.

Results: Eighty-two patients were included in the final analysis (Arm A: 40; Arm B: 42). The study was stopped for futility after interim analysis. Median overall survival (OS) was 9.38 months (95% CI: 5.0, 12.2) for Arm A and 14.7 months (95% CI: 11.6, 20.0) for Arm B (HR 1.75, p=0.019). Using immune related-response criteria, 2 partial responses (5.7%) were observed in Arm A and 4 (13.8%) in Arm B. GVAX + ipilimumab promoted T cell differentiation into effector memory phenotypes both in the periphery and in the tumor microenvironment and increased M1 macrophages in the tumor.

Conclusions: GVAX and ipilimumab maintenance therapy did not improve OS over continuation of chemotherapy and resulted in a numerically inferior survival in metastatic PDA. However, clinical responses and biological effects on immune cells were observed. Further study of novel combinations in the maintenance treatment of metastatic PDA is feasible.

Introduction

Pancreatic ductal adenocarcinoma (PDA) has a dismal prognosis. Affecting over 56,000 people in the US each year, incidence continues to rise, while 5-year survival rate remains at 10%(1). In the metastatic setting, multi-agent chemotherapy regimens have led to improved outcomes; however, eventual progression occurs and cumulative toxicities are significant (2, 3).

For the many patients with metastatic PDA who respond to but cannot tolerate multi-agent chemotherapy, such as FOLFIRINOX [5-fluorouracil, leucovorin, irinotecan, and oxaliplatin] beyond 4–6 months, the optimal approach is unknown. Two studies have recently reported results of different maintenance approaches after induction FOLFIRINOX. A “stop and go” strategy of maintenance leucovorin/5-fluorouracil after 4 months of induction FOLFIRINOX resulted in comparable survival to six months of FOLFIRINOX but actually increased neurotoxicity(4). The Pancreas Cancer Olaparib Ongoing (POLO) study led to the approval of olaparib, a poly ADP ribose polymerase (PARP) inhibitor, as maintenance therapy in patients with a germline BRCA1 or BRCA2 mutation and metastatic PDA whose disease had not progressed during first-line platinum-based chemotherapy(5).

Immunotherapy is attractive in the maintenance setting over chemotherapy given the general lack of cumulative bone marrow and neurologic toxicity, which can be rate-limiting in long term administration of chemotherapy. Furthermore, durable responses can be achieved in other diseases with the immune checkpoint inhibitors targeting cytotoxic T lymphocyte associated antigen 4 (CTLA-4) or programmed cell death-1 (PD-1); however, to date, no significant clinical activity of these agents has been observed in PDA(6–8). Combination with a vaccine may have the potential to convert “non-immunogenic” PDA into an immunogenic tumor through enhanced antigen presentation and priming of antigen-specific T cells(9–11). Granulocyte-macrophage colony-stimulating factor (GM-CSF)-secreting allogeneic pancreatic tumor cell (GVAX) immunotherapy consists of two irradiated human allogeneic pancreatic tumor cell lines modified to secrete GM-CSF, a cytokine that induces the maturation of dendritic cells. GVAX is a polyvalent source of tumor antigens, thereby

promoting T cell responses that diversify to multiple cancer antigens that are shared between the vaccine pancreatic tumor cell lines and patients' tumors. GVAX in combination with the CTLA-4 inhibitor, ipilimumab (IPI), showed promise in a previous phase 2 study in advanced PDA, with a 12-month overall survival (OS) of 27% vs. 7% and median OS of 5.7 months vs. 3.6 months for GVAX + IPI versus IPI alone, respectively(12).

We hypothesized that giving combination GVAX + IPI immediately after front-line chemotherapy in the maintenance setting, where patients are maximally debulked, may improve activity. We report herein the results of a multi-institutional phase 2 study evaluating GVAX + IPI as maintenance immunotherapy versus continuation of chemotherapy for patients with metastatic PDA who received initial FOLFIRINOX.

Patients and Methods

Study design

This was a multi-institutional, randomized, phase 2 study conducted at the Sidney Kimmel Comprehensive Cancer Center at Johns Hopkins University (Baltimore, Maryland), University of California San Francisco (UCSF) Medical Center (San Francisco, California), and Washington University School of Medicine (St. Louis, Missouri). Patients with metastatic PDA who had received 8–12 doses of FOLFIRINOX as part of standard therapy and had imaging evidence of response or stable disease were eligible. Randomization was stratified based on the number of prior FOLFIRINOX cycles (8 cycles or >8 cycles) and by center. Within each strata, patients were randomized 1:1 to GVAX + IPI (Arm A) or continued FOLFIRINOX (Arm B). The primary objective of the study was to compare overall survival (OS) between the two arms. Secondary objectives were to assess safety, characterize toxicities, and assess clinical and immunological responses. The study was reviewed by the local Institutional Review Boards and biosafety committees at each institution, the US Food and Drug Administration, and the National Institutes of Health Recombinant DNA Advisory Committee. The trial was conducted according to the Declaration of Helsinki and the Good Clinical Practice guidelines of the International Conference on Harmonization. All patients provided written informed consent prior to enrollment.

Patient Selection

Eligible patients had: histologically proven PDA; stable or responding metastatic disease after receiving 8–12 doses of FOLFIRINOX; age ≥18 years; Eastern Cooperative Oncology Group (ECOG) performance status of 0 or 1; normal organ and marrow function; and a life expectancy of >3 months. Key exclusions were: discontinuation of FOLFIRINOX more than 70 days prior to treatment on study, prior chemotherapy for metastatic pancreatic cancer (other than FOLFIRINOX), infection with HIV, hepatitis B or C; a history of brain metastases; radiographic ascites that was apparent on physical exam or requiring medical intervention; autoimmune disease; any known immune deficiencies; prior immunotherapy; or concomitant immunosuppressive agents.

Treatment and Assessments

Patients in Arm A received GVAX + IPI every 3 weeks for 4 induction doses, then every 8 weeks. GVAX treatment consisted of two irradiated, allogenic, GM-CSF-secreting pancreatic cancer cell lines (Panc 6.03 and Panc 10.05, at 2.5×10^8cells each; Johns Hopkins University, Baltimore, MD), combined and administered as a total of 6 intradermal injections. IPI was administered intravenously following GVAX. IPI was initially given at a dose of 10 mg/kg; patients who initiated treatment at this dose continued to receive subsequent doses at 10 mg/kg. However, the protocol was amended to decrease the IPI dose to 3 mg/kg for subsequent patients to improve tolerability. Patients in Arm B continued on FOLFIRINOX every 2 weeks if tolerated and were permitted to receive this treatment at an outside location; modifications to FOLFIRINOX were allowed.

Patients in Arm A were assessed prior to each treatment for safety. Adverse events (AEs) were graded according to the National Cancer Institute Common Terminology Criteria for Adverse Events (CTCAE) Version 4.0. All AEs experienced by patients in Arm A were collected and reported from the first dose and through 70 days after the last dose. Adverse events related to IPI and thought to be autoimmune in nature were designated as immune-related AEs (irAEs). AEs were not collected for patients in Arm B.

Radiographic assessments were performed at baseline, week 10, and then every 8 weeks. Responses were determined according to RECIST (version 1.1) and immune-related response criteria (irRC)(13, 14). Patients in Arm A were allowed to continue GVAX + IPI treatment up until the week 18 scan, even with progressive disease. Patients with disease progression on or after week 18 were discontinued from treatment. Patients in Arm B were treated until clinically significant disease progression as determined by the investigator.

Immunological assessments

Immune profiling of peripheral blood immune cells by mass cytometry—Paired peripheral blood lymphocytes (PBLs) from baseline and week 7 (after at least two doses of GVAX + IPI) from 20 patients in Arm A were available for analysis. Peripheral blood lymphocytes were subjected to mass cytometry analysis (cytometry by time-of-flight, CyTOF). Details of the panel of CyTOF antibodies used are tabulated (Supplementary Table S1). Using a combination of 3 of 5 unique metal isotopes (89Y, 113In, 115In, 194Pt, 198Pt) conjugated to CD45 antibodies, we then designed a barcoding strategy with 10 barcodes (5-choose-3) of anti-CD45 antibodies to yield 4 batches of 10 samples. Pooled samples were first blocked with Fc block (Invitrogen) for 10 minutes at room temperature (RT), stained for chemokine receptors for 10 minutes at 37°C, and then stained for the rest of the surface markers for 30 minutes at RT. After two washes, intracellular staining was performed using Cytofix/Cytoperm kit (BD Biosciences) per manufacturer's protocol. Cells were then stored in fresh 1% methanol-free formaldehyde in PBS (Thermo Scientific) until rhodium labeling (Fluidigm) at 1:1000 for 45 minutes at RT. All events were acquired on a Helios™ mass cytometer (Fluidigm).

For data analysis, samples were stratified based on disease status on the first restaging scan, with the "stable" cohort being defined as patients who demonstrated at least stable disease in

the first restaging scan and “progressive” cohort referring to patients who demonstrated progressive disease. Randomization, bead normalization, and bead removal of data collected were performed on CyTOF software (Fluidigm) v6.7. Using FlowJo (BD) v10.5, single cell events were identified by gating a tight population based on cell length and rhodium signal. After removing dead cells and debarcoding by manual gating, a computational pipeline based on diffcyt(15) was employed using R v3.5. For clustering the entire dataset based on shared protein expression across PBLs, the FlowSOM algorithm(16) was used to identify 40 meta-clusters that were then annotated into 23 final immune cell subtypes. Clustering was visualized using a two-dimensional uniform manifold approximation and projection (UMAP) dimensionality reduction algorithm(17) (Supplementary Figure S1). Analyses were performed across all cells and 2000 randomly selected cells per sample were used for visualization.

Multiplex immunohistochemistry (IHC)—Paired tumor biopsies were obtained at baseline and week 7 (after at least two doses of GVAX + IPI) in 6 patients on Arm A. A pathologist selected samples containing >30% tumor cellularity for 10-plex multiplex IHC. Multiplex IHC was conducted on 4 micron thick formalin fixed paraffin embedded (FFPE) tissue sections mounted on slides as previously described(18). Iterative staining was achieved by washing and antibody stripping in heated citrate (HK080–9K BioGenex, Fremont, CA). Samples were restained sequentially with antibodies indicated (Supplementary Table S2, Supplementary Figure S2.A).

Whole-slide scans were obtained after each stain on Hamamatsu Scanner at 20x magnification. Digital image analysis consisted of three steps: 1) image coregistration using Cell Profiler 2 (Version 2.2.0, Broad Institute) with “coregistration 12 markers” pipeline, 2) visualization in ImageJ Version 2 (Java 1.8.0_172 (64-bit), NIH), and 3) quantitative image analysis of staining intensity was performed in three areas per FFPE tissue ($\geq 6.25 mm^2$) using Cell Profiler 2 with “cytometry 12 markers” pipeline and FlowFCS Express 6 Image Cytometry Version 6.06.022 (De Novo Software) (Supplementary Figure S2). Images were merged in Halo (version 2.0.1145.31, Indica labs) to identify immune subsets according to lineage markers described (Supplementary Table S3).

Statistical considerations

Clinical Trial Analyses—A sample size of 92 patients (46 per arm) was chosen to give 82% power with a 1-sided type 1 error rate of 10% to detect an increase in proportion alive at 6 months (0.68 for GVAX + IPI compared to a null of 0.53 for continued FOLFIRINOX). An interim futility analysis was planned once 50% of the information was available (i.e. after approximately 38 deaths were observed).

Baseline characteristics are summarized overall and within each treatment group. For continuous variables, the median and first to 3rd quartile is included. For categorical variables, the count and proportion within each category is included. AEs are summarized using counts and proportions.

Overall survival is defined as the time from randomization until the death. Kaplan-Meier estimates of the survival function were computed and used to estimate the median overall

survival with 95% confidence intervals (CI) and to display the comparison between groups graphically. Cox proportional hazards models were used to compare the overall survival between treatment groups as well as the heterogeneity of the treatment effect within subgroups of interest. The overall survival was compared for the two doses of IPI (10 mg/kg and 3 mg/kg) to determine whether the effect of GVAX + IPI was heterogeneous.

Progression free survival (PFS) is defined as the time from randomization to progression. Immune-related progression free survival (irPFS) is defined as the time from randomization to immune-related progression. Individuals who died within 3 months of the last scan were counted as having progressed. Otherwise, individuals without follow-up scans were censored one day after randomization and individuals with follow-up scans were censored at the date of the last scan. PFS and irPFS were analyzed using the same technique as OS.

Correlative Studies Analyses—Associations between immune parameters were explored graphically (e.g. scatterplots, boxplots) and numerically (e.g. correlations, χ^2 tests). For differential analyses of the CyTOF dataset, negative binomial methodology was used for cell type abundance comparisons (edgeR) and linear mixed modeling was used for mean marker intensity comparisons (limma)(19, 20) implemented in the diffcyt framework(15). The final model for differential analyses incorporated random batch effects. FDR adjusted p values were used to account for multiple hypothesis testing using R packages. Two-way ANOVA was performed for each cell type to test whether the clinical outcome interacted with the effect of GVAX + IPI treatment on cell type abundances.

For analyses of multiplex IHC biomarker expression on FFPE metastatic PDA biopsy tissue, comparisons of cell percentages among cell lineages were determined using Student's t-tests. P values <0.05 indicate statistical significance. All statistical analyses used GraphPad Prism (version 8.0.2, GraphPad Software, Inc, La Jolla, CA).

Results

Patient Characteristics, Safety, and Tolerability

Between December 2013 and January 2017, a total of 83 patients were randomized (Figure 1). One patient in Arm A assigned to receive 3mg/kg of IPI was lost to follow up prior to receiving treatment and was therefore excluded from analyses. The remaining 82 patients were included in the response analysis: 40 Arm A and 42 Arm B. In general, patients appeared similar between arms; however, more patients in Arm A had peritoneal involvement and CA 19–9 ≥ 59 times the upper limit of normal (Table 1).

A total of 39 out of 40 Arm A patients received at least one dose of study drug. The remaining Arm A patient was randomized but came off study for progression prior to initiating study treatment and was excluded from the toxicity analysis. Due to toxicity concerns, the dose of IPI was reduced from 10mg/kg to 3mg/kg during the course of the study. Twenty-five patients were treated with IPI at 10 mg/kg (IPI10) and 14 with IPI at 3 mg/kg (IPI3). The participant who progressed prior to initiating treatment was recruited prior to the dose change. Treatment-related adverse events (TRAEs) are summarized in Supplementary Table S4. Grade ≥3 AEs related to study drugs (i.e. rash, colitis,

pneumonitis, hepatitis, and endocrinopathies) occurred in 36% of patients treated at IPI3 and 44% of patients treated at IPI10. Only 1 Grade 4 TRAE (pneumonitis) was observed. Adverse events attributed to GVAX were all mild (≤ grade 2) and were primarily local vaccine site reactions. Fever and fatigue were also frequently reported. Patients were permitted to continue GVAX if ipilimumab was discontinued for toxicity. Only one patient elected to discontinue study participation due to toxicity, which was rash and adrenal insufficiency related to study drug.

Seven patients on Arm B withdrew after randomization to receive a different treatment. Chemotherapy regimens administered to the remaining 35 patients are summarized (Supplementary Table S5). Fourteen patients continued to receive FOLFIRINOX, 13 received FOLFIRI, 2 received FOLFOX, and 6 received 5FU/LV or capecitabine as maintenance.

Response and survival

At the time of interim futility analysis, a total of 46 deaths had occurred. The study was closed to enrollment as overall survival was significantly lower for Arm A compared to Arm B (Hazard Ratio [HR]: 1.85, 95% Confidence Interval [CI]:1.03–3.33, p = 0.036). The final analysis included 82 patients and 72 deaths (38 in Arm A; 34 in Arm B). The median overall survival (OS) was 9.38 months (95% CI: 5.0–12.2) in Arm A versus 14.7 months (95% CI: 11.6–20.0) in Arm B (HR: 1.75 95% CI: 1.09–2.79, p=0.019) (Figure 2A). Time from diagnosis of metastatic disease, time on treatment, time to progression, and overall survival are displayed graphically for individual subjects in both Arms in Supplementary Figure S3. Subgroup analysis did not reveal any subsets in which Arm A treatment was favored (Figure 2B). There were no apparent differences in outcome according to dose of IPI. Median OS was 9.45 months (95% CI: 5.06–13.9) in the IPI3 cohort, and 8.08 months (95% CI: 4.17–15.9) in the IPI10 cohort (HR: 0.89, 95% CI: 0.44–1.76, p = 0.73). Median PFS was 2.4 months (95% CI: 1.87–2.53) in Arm A versus 5.55 months (95% CI: 3.32–8.51) in Arm B (HR: 2.92, 95% CI: 0.1.70–5.02, p<0.001) with 65% and 91% alive at 6 months, respectively. Similarly, the irPFS was shorter in Arm A than in Arm B (median: 2.50 vs 5.55, HR: 3.05, 95% CI: 1.74–5.35, p < 0.001).

Patients who came off study before their first follow-up scan (1 in Arm A and 7 in Arm B) and those with no measurable disease at baseline (4 in Arm A and 6 in Arm B) were excluded from response rate analysis. Disease control rate (PR+SD) analysis excluded only patients without follow-up scans. Among the remaining patients, best response of partial response (PR) by RECIST 1.1 was observed in 1 patient (2.9%) in Arm A and 3 patients (10.3%) in Arm B. 11 patients in Arm A versus 24 patients in Arm B had a best response of stable disease (SD). The disease control rate was 30.8% in Arm A and 77.1% in Arm B. By irRC, 2 PRs (5.7%) were observed in Arm A and 4 (13.8%) in Arm B. The disease control rate by irRC was 38.5% in Arm A and 80% in Arm B. CT findings demonstrated early tumor growth at week 10 followed by regression at week 18 in the Arm A patient with a PR (Figure 3).

Analysis of Peripheral Blood Lymphocytes

To profile the peripheral immunologic response to treatment, we performed mass cytometry (CyTOF) analysis using a panel focused on T cell phenotyping (15 subtyping, 9 functional, and 3 cytokine markers) on PBLs collected at baseline and on-treatment in 20 Arm A patients.

We first examined the effect of GVAX + IPI on the relative abundance of immune subtypes as a percentage of $CD45^+$ cells individually (Supplementary Figure S1) and for all of the patients stacked via radar plot (Figure 4A). Comparing baseline and on-treatment profiles, GVAX + IPI treatment was associated with decreases in naive T helper cells (Th N) and increases in T helper effector memory cells (Th EM) from baseline. Although less in magnitude, there were also significant increases in effector memory cytotoxic T cells (Tc EM) with decreases in the naïve cytotoxic T cells (Tc N). There was no obvious difference in the abundance of the other T cell subsets or B cells after immunotherapy. Furthermore, these changes were noted regardless of disease status on the first restaging scan, i.e. progressive vs. stable; the clinical outcome did not significantly correlate with the effect of GVAX + IPI on any of the cell type abundances ($p>0.05$ for all two-way ANOVA).

We next analyzed the functional states of immune subsets before and after GVAX + IPI treatment by comparing the expression levels of co-stimulatory markers (CD28, 41BB, OX40), proliferation (Ki67), a serine protease effector molecule (granzyme B), cytokines (IL-2, IFNγ, TNFα), and co-inhibitory markers (PD-1, TIM3, CTLA-4, LAG3). Again, the effect of treatment on the expression of functional markers within each of the cell clusters did not correlate with disease response (all FDR-adjusted p values >0.05, Supplementary Figure S4). Thus, we focused our analysis on comparing the functional states before and after treatment with GVAX + IPI.

When looking at co-stimulatory or activation markers and expression of CD28 and Ki67 in several helper and cytotoxic T cell clusters, both effector and effector memory states increased significantly with GVAX + IPI (Figure 4B, Supplementary Figure S4). Moreover, GVAX + IPI therapy led to increased CD28 expression in both cytotoxic and helper T type 17 cells (Tc17 and Th17), which are characterized by high expression of CCR6 and CXCR3 (21, 22). In Th17 cells, this was again accompanied by increased Ki67. Production of IL-2 in effector memory helper T cell clusters (Th EM 1, 2, 3) and one effector memory cytotoxic T cell cluster (Tc EM 3) was also enhanced by treatment (Supplementary Figure S4). As expected, we noted high granzyme B expression in cytotoxic T effector and effector memory cells, Tc17, and NK cells both at baseline and on-treatment; there was no change in expression related to treatment. There were also high levels of TNFα and IFNγ expression in cytotoxic effector T cells both at baseline and on-treatment.

Among the co-inhibitory markers assayed, we found that GVAX + IPI notably upregulated the expression of TIM3 in most helper and cytotoxic T cell clusters and PD-1 in some (Figure 4B, Supplementary Figure S4). The expression of CTLA4 was largely maintained with treatment, with mild increases in effector memory clusters.

To evaluate whether baseline T cell states correlated with clinical outcomes, we enumerated the list of functional markers that had at least a 15% fold difference on average when comparing patients with best response of stable versus progressive disease (Supplementary Table S6). High expression of IL-2 in effector memory cytotoxic T cells at baseline was the only functional state at baseline that significantly correlated with stable disease (1.19-fold higher; FDR adjusted p values <0.05). From a discovery point-of-view (non-FDR adjusted p values <0.05), baseline functional states that correlated with stable over progressive disease included higher expression of TNFα in early differentiating helper T cell clusters (naïve and central memory), IFNγ in effector and naïve cytotoxic T cells, and Ki67 in IFNγ-high effector memory T cells (Tc EM4).

Analysis of Tumor Biopsies

Metastatic pancreatic tumor biopsies were obtained in 16 patients at baseline and 6 patients on-treatment in Arm A only. To profile the immunologic response to GVAX + IPI in the tumor, we performed multiplex IHC analysis using a T cell and myeloid cell-focused panel on the 6 sets of paired biopsies. Of these 6 patients, 2 had a best response of stable disease and 4 had progressive disease.

Changes in immune cell subsets were quantified as a percentage of $CD45^+$ cells (Figure 5A). This analysis revealed a statistically significant increase in $CD8^+$ T cells and M1 macrophages, a decrease in M2 macrophages, and the suggested decrease in $FoxP3^+$ T regulatory cells, although the last was not statistically significant. Image visualization by pseudocoloring of baseline and on-treatment FFPE sections of two representative areas in tumor biopsies taken from a patient who achieved a best response of stable disease are shown (Figure 5B–D), illustrating an increase in frequency of $CD45^+CD4^+$ T helper cells and $CD45^+CD8^+$ cytotoxic T cells, decrease in $CD45^+CD4^+Foxp3^+$ T regulatory cells, and increase in $CD45^+CSF1R^+CD68^+CD163^-$ M1 macrophages but decrease in $CD45^+CSF1R^+CD68^+CD163^+$ M2 macrophages in the tumor microenvironment after GVAX + IPI treatment.

We were interested in the functional profile of $CD45^+CD8^+$ T cells, and therefore, we evaluated the PD-1 and EOMES status and the percentages of functional T cell subtypes at baseline and on-treatment. We found that GVAX + IPI elicited a decrease in early effector ($EOMES^+PD\text{-}1^-$) $CD8^+$ T cells and exhausted ($EOMES^+PD\text{-}1^+$) $CD8^+$ T cells and an increase in late effector ($EOMES^-PD\text{-}1^+$) $CD8^+$ T cells and memory ($EOMES^-PD\text{-}1^-$) $CD8^+$ T cells from baseline independent of clinical outcome (Figure 5E). The small sample size limited our ability to correlate these findings with clinical outcomes.

Discussion

PDA is characterized by a low tumor mutation burden and a uniquely immunosuppressive tumor microenvironment, both of which likely contribute to the lack of effective anti-tumor immunity and lack of significant clinical activity of the immune checkpoint inhibitors targeting CTLA-4 or PD-1(23–26). Thus, a multi-pronged strategy to prime and expand tumor antigen-specific T cells and block negative immune checkpoints is hypothesized to be necessary to induce an effective anti-tumor immune response. In this study, we evaluated the

combination of GVAX + IPI as maintenance treatment for patients with metastatic PDA who responded to front-line FOLFIRINOX. To our knowledge, this is the first such study to report results of immunotherapy in the maintenance setting for metastatic PDA. In general, toxicity rates were comparable to what has been seen for these agents(12, 27). Notably, we did observe a numerically higher rate of TRAEs with the IPI10 dosing, particularly with regard to the gastrointestinal toxicity as has been reported previously(28). There was no apparent dose effect on the clinical activity of the combination.

The study did not meet the primary endpoint of improvement in OS with GVAX + IPI maintenance treatment over continuation of FOLFIRINOX. Survival was shorter with the experimental regimen. However, our results are remarkable for several reasons. First, the survival in both cohorts was longer than expected, suggesting that patients entering maintenance are a highly selected group with a biology that differs from those who do not become eligible for maintenance. To our knowledge, there is limited published data on survival in this setting. We assumed a 6-month OS rate of 53% for patients who continue FOLFIRINOX based upon the Conroy study, but we observed a much higher rate of 91%, as well as 65% with GVAX + IPI. The lower than expected rate of liver metastases as well as high proportion of patients with prior resection do support patient selection as a contributing factor to the better than expected outcomes. Second, response rates may not be a good measure in debulked patients. Third, to our knowledge, this is the only study in the maintenance setting to use continuation of multi-agent chemotherapy as the comparator rather than single agent chemotherapy or placebo. The study, by design, selected a patient population sensitive to chemotherapy, and then continued active chemotherapy in the comparator. The results suggest that this approach may have beneficial clinical effect. These first two findings, provide new assumptions, which can provide the backbone for future maintenance studies.

We demonstrated several alterations in the immune response both in the periphery and intratumorally in patients treated with GVAX + IPI, suggesting a biologic effect of this regimen and the potential for further optimization to induce effective anti-tumor immunity. Analysis of pre- and on-treatment peripheral blood samples by CyTOF demonstrated that GVAX + IPI treatment yields successful systemic immunologic responses regardless of the clinical outcome, strongly promoting T cell differentiation into effector memory phenotypes from naïve T cells. Given that GVAX + IPI had little effect on the CTLA-4 expression levels, but rather upregulated alternative checkpoints TIM3 and PD-1 in these T cell subsets, the results suggest that while GVAX + IPI successfully elicits increased differentiation and activation of multiple T cell subsets, such pro-immune effects were accompanied by compensatory increases in alternative pathways of exhaustion. These compensatory increases could provide targets for the next generation of studies. Interestingly, certain baseline T cell states, but not the degrees of change in the T cell states after GVAX + IPI, were more associated with stable disease on CT scan. For instance, high expression of IL-2 in effector memory cytotoxic T cells at baseline was significantly correlated with stable disease, suggesting that patients with higher levels of pro-inflammatory cytokine production in T cells, characterized at the systemic level, may be immunologically poised to suppress tumor growth upon treatment with immunotherapy. This adds to our prior studies of the T cell repertoire in patients treated with GVAX + IPI, which showed expansion in T cell

repertoire in response to treatment, with higher clonality after treatment associated with the longest survival(12, 29).

While analysis of the tumor microenvironment was more limited in this study due to small numbers of paired biopsies, this may be a general limitation of maintenance studies particularly with regards to tissue collection, as patients may have been “debulked” by chemotherapy. Fortunately, the advent of multiplex IHC technology has allowed us to preserve precious tissue specimen and visualize better co-localization of different markers on individual cells. The immune changes observed in the tumor appeared similar to what was seen in the periphery. Specifically, we noted increases in CD4+ T helper cells in the metastatic tumor in the same patients that showed increases in CD4+ T helper effector memory cells in their blood. Although less in magnitude, there were also increases in late effector and memory cytotoxic T cells in the metastatic tumor that were also observed in the peripheral blood lymphocytes of the same patients. However, these correlations are based on a small number of patients. Furthermore, it would be more valuable to characterize the accompanying repertoire of these T cells present in the tumor microenvironment before and after combination GVAX + IPI immunotherapy via T cell receptor sequencing. Of note, the feasibility and robustness of such analysis would depend on the availability of T cells that can be enriched from the biopsy samples, regarding which this study is limited. In addition, we observed an increase in pro-inflammatory M1 macrophages and decrease in pro-tumorigenic M2 macrophages in the tumor. Altogether, these results suggest that GVAX + IPI treatment significantly yields successful local immunologic responses and promotes a decrease in immunosuppressive cells in the metastatic PDA tumor microenvironment.

A worthwhile addition to the current study would have been the analysis of longitudinal immune correlates in the chemotherapy control arm upon which to base comparisons of our findings. While collection of on-treatment research samples was planned for patients in Arm B, these subjects were permitted to receive chemotherapy at an outside location and therefore the majority did not return for this. Given that these patients had received at least 4 months of FOLFIRINOX prior to enrollment and were to continue on this regimen, we did not anticipate dynamic changes in their immune compartments peripherally or intratumorally. An unanswered question is how the changes we observed with GVAX + IPI compare to what would be seen with no treatment.

In summary, the strong systemic and intratumoral activation of T cells in patients from baseline to post-immunotherapy treatment and upregulation of non-CTLA-4 checkpoint markers on specific peripheral T cell subsets support the concept that giving GVAX immunotherapy may be inducing activation of naïve T cells to antigen-specific T cells. Meanwhile, ipilimumab blocks CTLA-4, which improves priming of T cells, but also upregulates additional T cell activation and regulatory markers as a compensatory mechanism. Since activation by GVAX + IPI does not translate into improved clinical responses, it is likely that these negative feedback pathways are not overcome by GVAX + IPI alone. While our analysis specifically demonstrated upregulation of PD-1 and TIM3 signaling during therapy, other speculated pathways not assessed in this study include stromal barriers or suppressive cytokines that prevent immune cells from entering the tumor microenvironment and exerting their antitumor effects. This clinical trial highlights the

challenges to therapeutically inducing an effective anti-tumor immune response in PDA with multiple counterregulatory mechanisms. Ongoing and future studies are building on this work by examining GVAX with a listeria-based mesothelin vaccine and immune checkpoint inhibitors in combination with other immune and stromal modulating agents in metastatic pancreatic ductal adenocarcinoma. Furthermore, this work sheds light on potential predictive biomarkers that can allow for better patient selection to identify those most likely to benefit from a given immunotherapy.

Supplementary Material

Refer to Web version on PubMed Central for supplementary material.

Acknowledgements

We gratefully acknowledge the patients who participated in this trial and their families. We also thank University of Maryland School of Medicine Center for Innovative Biomedical Resources Flow and Mass Cytometry Core Facility in Baltimore, Maryland for services related to mass cytometry data acquisition. Kelly Gemmill assisted in manuscript preparation.

Financial support

D.T.L. and E.M.J were funded by FDA/R01 (1RO1FD004819), NCI/NIH Spore in Gastrointestinal Cancer (P50CA062924 and CA62924), and the Viragh Family Foundation's Pancreatic Cancer Fund. E.M.J was also funded by the Broccoli Foundation and the Emerson Collective Cancer Research Fund.

References

1. Howlader N, Noone AM, Krapcho M, Miller D, Brest A, Yu M, et al. SEER Cancer Statistics Review, 1975–2017, National Cancer Institute. Bethesda, MD,.
2. Conroy T, Desseigne F, Ychou M, Bouche O, Guimbaud R, Becouarn Y, et al. FOLFIRINOX versus gemcitabine for metastatic pancreatic cancer. N Engl J Med. 2011;364(19):1817–25. [PubMed: 21561347]
3. Von Hoff DD, Ervin T, Arena FP, Chiorean EG, Infante J, Moore M, et al. Increased survival in pancreatic cancer with nab-paclitaxel plus gemcitabine. N Engl J Med. 2013;369(18):1691–703. [PubMed: 24131140]
4. Dahan L, Phelip JM, Malicot KL, Williet N, Desrame J, Volet J, et al. FOLFIRINOX until progression, FOLFIRINOX with maintenance treatment, or sequential treatment with gemcitabine and FOLFIRI.3 for first-line treatment of metastatic pancreatic cancer: A randomized phase II trial (PRODIGE 35-PANOPTIMOX). Journal of Clinical Oncology. 5 20, 2018;36(no. 15_suppl):4000-.
5. Golan T, Hammel P, Reni M, Van Cutsem E, Macarulla T, Hall MJ, et al. Maintenance Olaparib for Germline BRCA-Mutated Metastatic Pancreatic Cancer. N Engl J Med. 2019;381(4):317–27. [PubMed: 31157963]
6. Royal RE, Levy C, Turner K, Mathur A, Hughes M, Kammula US, et al. Phase 2 trial of single agent Ipilimumab (anti-CTLA-4) for locally advanced or metastatic pancreatic adenocarcinoma. J Immunother. 2010;33(8):828–33. [PubMed: 20842054]
7. Brahmer JR, Tykodi SS, Chow LQ, Hwu WJ, Topalian SL, Hwu P, et al. Safety and activity of anti-PD-L1 antibody in patients with advanced cancer. N Engl J Med. 2012;366(26):2455–65. [PubMed: 22658128]
8. O'Reilly EM, Oh D-Y, Dhani N, Renouf DJ, Lee MA, Sun W, et al. A randomized phase 2 study of durvalumab monotherapy and in combination with tremelimumab in patients with metastatic pancreatic ductal adenocarcinoma (mPDAC): ALPS study. Journal of Clinical Oncology 36, no 4_suppl (2 01, 2018) 217–217. [PubMed: 29161205]

9. Lutz ER, Wu AA, Bigelow E, Sharma R, Mo G, Soares K, et al. Immunotherapy converts nonimmunogenic pancreatic tumors into immunogenic foci of immune regulation. Cancer Immunol Res. 2014;2(7):616–31. [PubMed: 24942756]
10. Quezada SA, Peggs KS, Curran MA, Allison JP. CTLA4 blockade and GM-CSF combination immunotherapy alters the intratumor balance of effector and regulatory T cells. J Clin Invest. 2006;116(7):1935–45. [PubMed: 16778987]
11. van Elsas A, Hurwitz AA, Allison JP. Combination immunotherapy of B16 melanoma using anti-cytotoxic T lymphocyte-associated antigen 4 (CTLA-4) and granulocyte/macrophage colony-stimulating factor (GM-CSF)-producing vaccines induces rejection of subcutaneous and metastatic tumors accompanied by autoimmune depigmentation. J Exp Med. 1999;190(3):355–66. [PubMed: 10430624]
12. Le DT, Lutz E, Uram JN, Sugar EA, Onners B, Solt S, et al. Evaluation of ipilimumab in combination with allogeneic pancreatic tumor cells transfected with a GM-CSF gene in previously treated pancreatic cancer. J Immunother. 2013;36(7):382–9. [PubMed: 23924790]
13. Eisenhauer EA, Therasse P, Bogaerts J, Schwartz LH, Sargent D, Ford R, et al. New response evaluation criteria in solid tumours: revised RECIST guideline (version 1.1). Eur J Cancer. 2009;45(2):228–47. [PubMed: 19097774]
14. Wolchok JD, Hoos A, O'Day S, Weber JS, Hamid O, Lebbe C, et al. Guidelines for the evaluation of immune therapy activity in solid tumors: immune-related response criteria. Clin Cancer Res. 2009;15(23):7412–20. [PubMed: 19934295]
15. Weber LM, Nowicka M, Soneson C, Robinson MD. diffcyt: Differential discovery in high-dimensional cytometry via high-resolution clustering. Commun Biol. 2019;2:183. [PubMed: 31098416]
16. Van Gassen S, Callebaut B, Van Helden MJ, Lambrecht BN, Demeester P, Dhaene T, et al. FlowSOM: Using self-organizing maps for visualization and interpretation of cytometry data. Cytometry A. 2015;87(7):636–45. [PubMed: 25573116]
17. Becht E, McInnes L, Healy J, Dutertre CA, Kwok IWH, Ng LG, et al. Dimensionality reduction for visualizing single-cell data using UMAP. Nat Biotechnol. 2018.
18. Tsujikawa T, Kumar S, Borkar RN, Azimi V, Thibault G, Chang YH, et al. Quantitative Multiplex Immunohistochemistry Reveals Myeloid-Inflamed Tumor-Immune Complexity Associated with Poor Prognosis. Cell Rep. 2017;19(1):203–17. [PubMed: 28380359]
19. Robinson MD, McCarthy DJ, Smyth GK. edgeR: a Bioconductor package for differential expression analysis of digital gene expression data. Bioinformatics. 2010;26(1):139–40. [PubMed: 19910308]
20. Smyth GK, Smyth GK. Limma: linear models for microarray data. In Bioinformatics and computational biology solutions using R and Bioconductor. Ed BY Gentlem R, CAREY V, DUDOIT S, IRIZARRY R, HUBER W.
21. Liu X, Zawidzka EM, Li H, Lesch CA, Dunbar J, Bousley D, et al. RORgamma Agonists Enhance the Sustained Antitumor Activity through Intrinsic Tc17 Cytotoxicity and Tc1 Recruitment. Cancer Immunol Res. 2019;7(7):1054–63. [PubMed: 31064778]
22. Knochelmann HM, Dwyer CJ, Bailey SR, Amaya SM, Elston DM, Mazza-McCrann JM, et al. When worlds collide: Th17 and Treg cells in cancer and autoimmunity. Cell Mol Immunol. 2018;15(5):458–69. [PubMed: 29563615]
23. Yarchoan M, Albacker LA, Hopkins AC, Montesion M, Murugesan K, Vithayathil TT, et al. PD-L1 expression and tumor mutational burden are independent biomarkers in most cancers. JCI Insight. 2019;4(6).
24. Yarchoan M, Hopkins A, Jaffee EM. Tumor Mutational Burden and Response Rate to PD-1 Inhibition. N Engl J Med. 2017;377(25):2500–1. [PubMed: 29262275]
25. Ino Y, Yamazaki-Itoh R, Shimada K, Iwasaki M, Kosuge T, Kanai Y, et al. Immune cell infiltration as an indicator of the immune microenvironment of pancreatic cancer. Br J Cancer. 2013;108(4):914–23. [PubMed: 23385730]
26. Feig C, Gopinathan A, Neesse A, Chan DS, Cook N, Tuveson DA. The pancreas cancer microenvironment. Clin Cancer Res. 2012;18(16):4266–76. [PubMed: 22896693]

27. Laheru D, Lutz E, Burke J, Biedrzycki B, Solt S, Onners B, et al. Allogeneic granulocyte macrophage colony-stimulating factor-secreting tumor immunotherapy alone or in sequence with cyclophosphamide for metastatic pancreatic cancer: a pilot study of safety, feasibility, and immune activation. Clin Cancer Res. 2008;14(5):1455–63. [PubMed: 18316569]

28. Wolchok JD, Neyns B, Linette G, Negrier S, Lutzky J, Thomas L, et al. Ipilimumab monotherapy in patients with pretreated advanced melanoma: a randomised, double-blind, multicentre, phase 2, dose-ranging study. Lancet Oncol. 2010;11(2):155–64. [PubMed: 20004617]

29. Hopkins AC, Yarchoan M, Durham JN, Yusko EC, Rytlewski JA, Robins HS, et al. T cell receptor repertoire features associated with survival in immunotherapy-treated pancreatic ductal adenocarcinoma. JCI Insight. 2018;3(13).

Statement of Translational Relevance:

While GVAX and ipilimumab was associated with numerically inferior survival relative to continuation of chemotherapy in the maintenance treatment of patients with non-biomarker selected, metastatic pancreatic adenocarcinoma, the combination did produce a response rate of 5.7%, disease control rate of 38.5%, and a median survival of 9.38 months. Furthermore, clear biologic effects on peripheral and intratumoral immune cells were observed. Changes in the periphery included increases in T cell activation markers, peripheral T helper and cytotoxic effector memory cells and decreases in naïve cytotoxic T cells. Interrogation of the tumor microenvironment revealed an increase in the M1 macrophage compartment and mirrored the peripheral blood changes with increases in late effector and memory T cells. The study of novel agents in this maintenance space was feasible and further studies are encouraged to fill this unmet medical need.

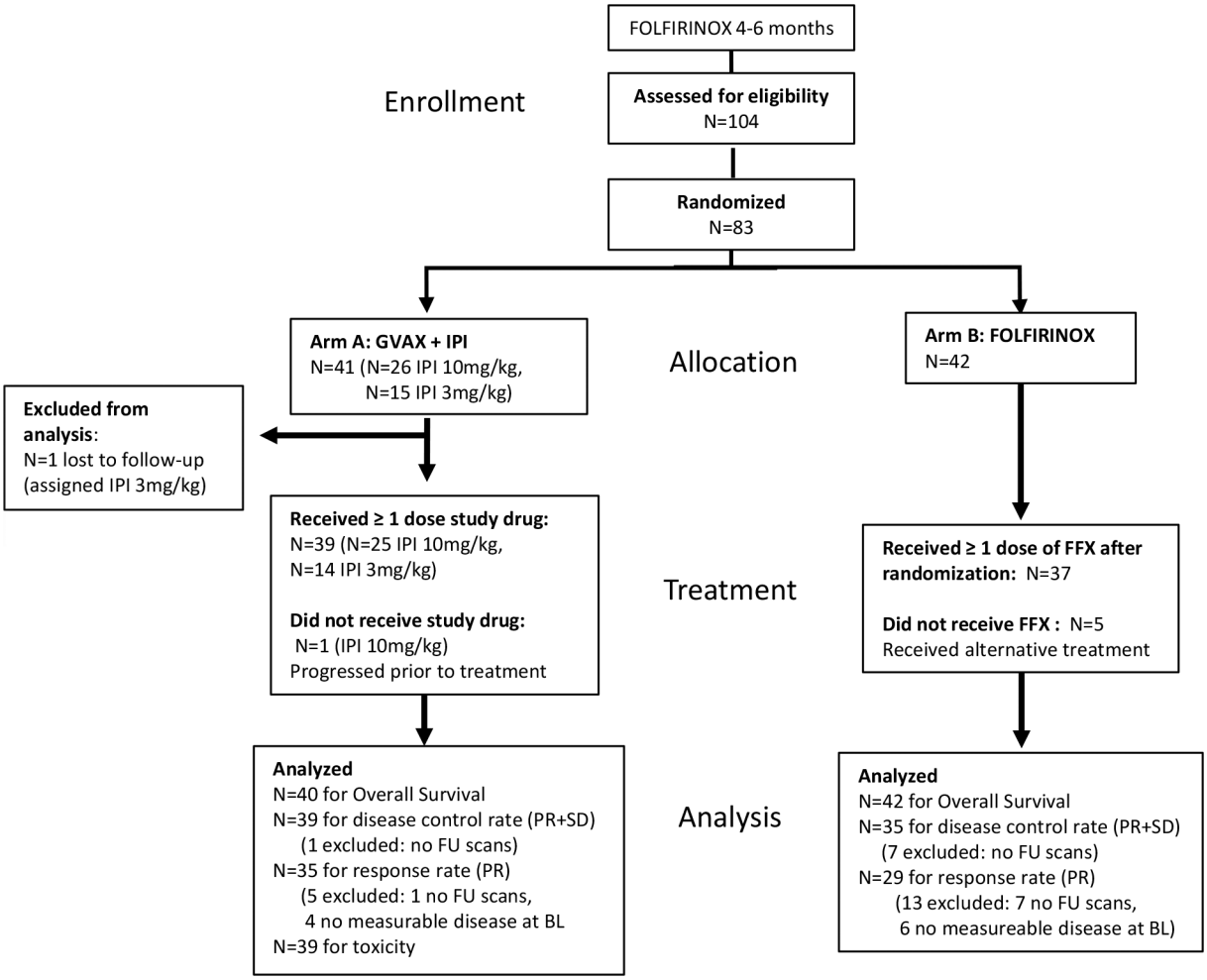

Figure 1. Consort diagram.

A diagram showing the enrollment of patients with metastatic pancreatic adenocarcinoma who were debulked with FOLFIRINOX chemotherapy, their allocation to treatment into Arm A versus Arm B treatment groups, disposition status, and how patients were analyzed in the trial.

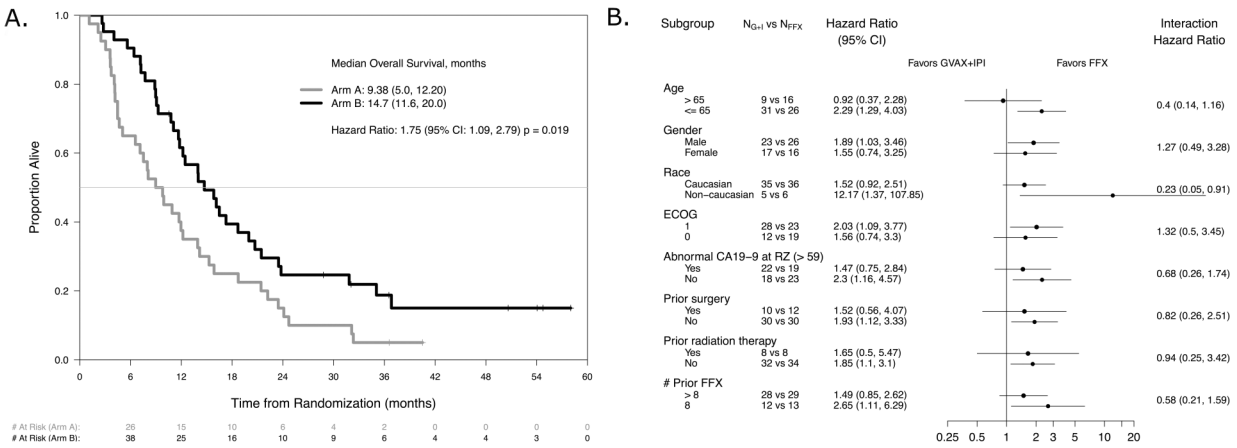

Figure 2. Patient survival and Subgroup analyses.

A. Overall survival. A comparison of overall survival in months for Arm A versus Arm B cohorts. Overall survival is calculated as the date of death or last follow-up minus date of randomization/30.4375. **B. Subgroup Analyses.** Forest plot of the treatment effect within subgroups defined by baseline demographic, disease, and treatment characteristics. N_A and N_B represent the number within each subgroup in Arm A and Arm B, respectively. Both the hazard ratio within each subgroup and the hazard ratio of the interaction comparing the subgroups are provided.

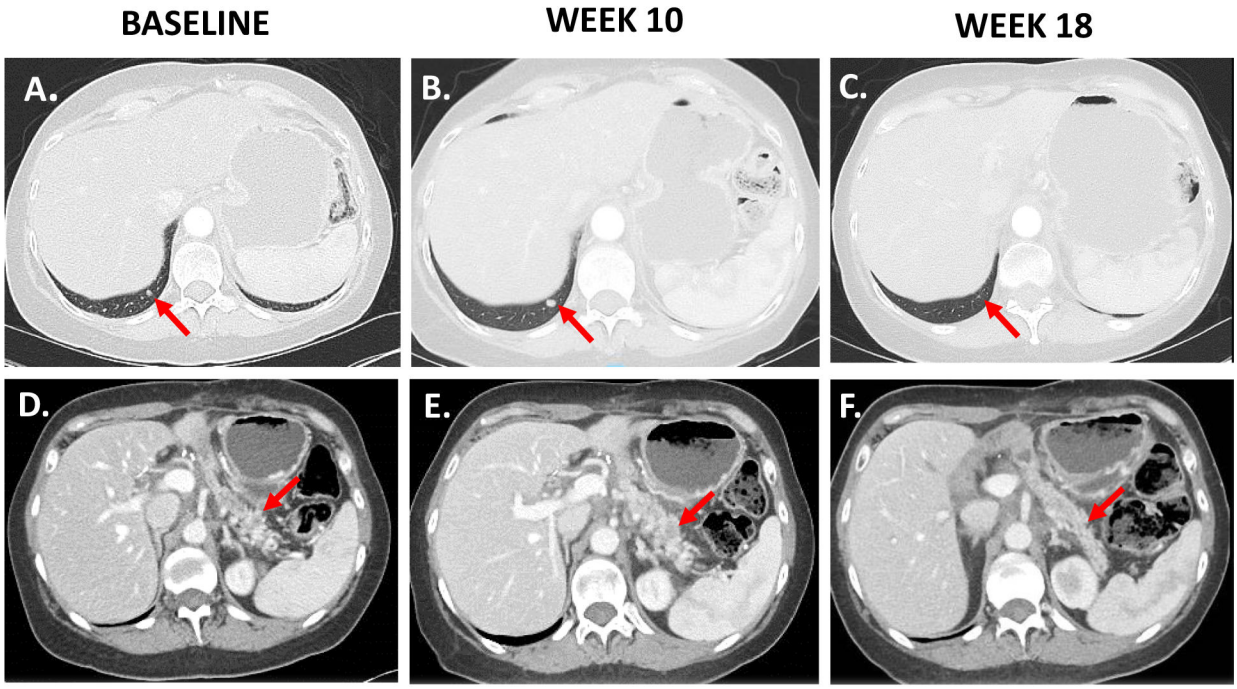

Figure 3. Delayed tumor responses shown radiographically in Arm A patient.

A and D. Baseline images of pancreas tumor in Arm A patient taken by CT scan in the axial plane. Red arrow points to tumor. **B and E.** Week 10 image shows tumor growth from baseline on CT scan. **C and F.** Week 18 image shows delayed tumor response on CT scan.

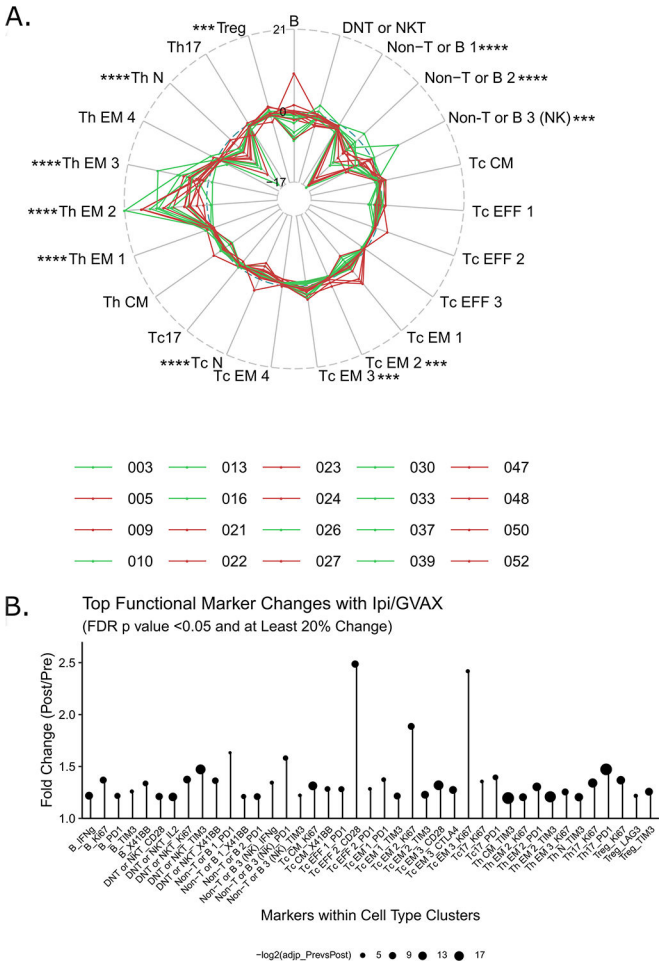

Figure 4. GVAX + IPI promotes differentiation towards memory away from naïve in peripheral T cells and induces changes in functional states of immune cell subsets.

A. Radar plots of progressive and stable disease cohorts show the difference in proportion of various T cell lineages between week 7 and baseline samples for individual patients. Each line represents one patient in Arm A (red: progressive; green: stable). Immune cell subsets are given their own axis. The numbers along the axes represent a change in abundance as a percentage of $CD45^{+}$ cells. FDR-adjusted p values from edgeR comparing pre- and post-treatment conditions are shown: *<0.05, **<0.01, ***<0.005, ****<0.0005. **B.** Only the markers that have changed at least 20% compared to the baseline mean metal intensity (MMI) with FDR p values <0.05 are plotted. Cell clusters are listed along the horizontal axis, and fold-changes in MMI (post/pre) are shown along the y-axis. There were no markers that have significantly decreased by more than 20%. Dot sizes represent–log2 of FDR-adjusted p values resulting from linear mixed modeling.

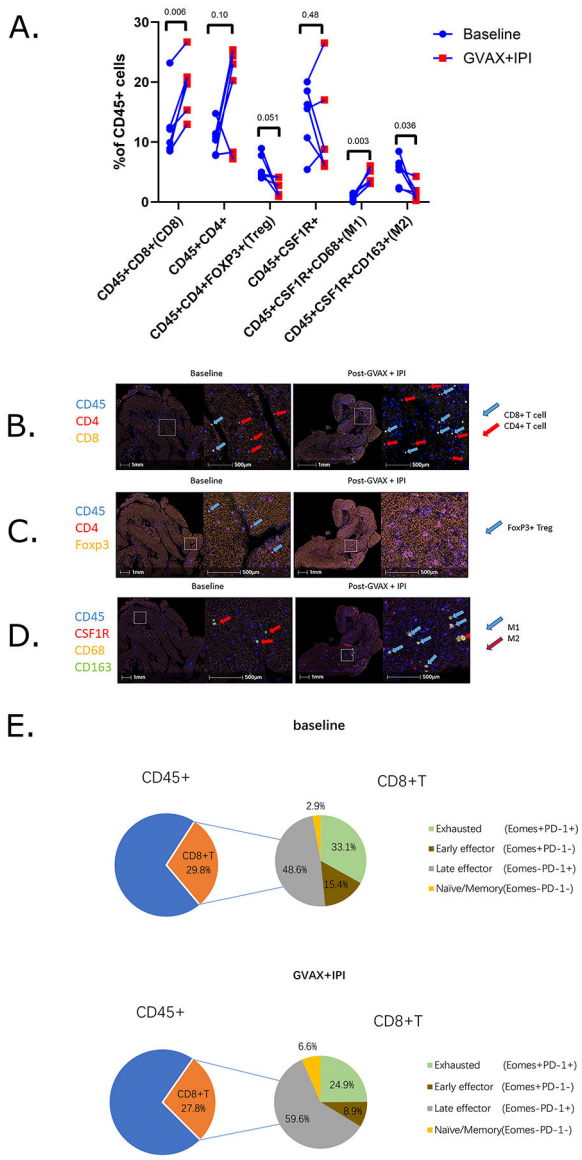

Figure 5. GVAX + IPI promotes an immunostimulatory phenotype in the metastatic pancreatic tumor microenvironment.

A. Longitudinal changes of immune cell composition of $CD45^+$ leukocyte cell densities from baseline (blue circle) to week 7 GVAX + IPI (red square). P values <0.05 indicates statistical significance; Student's t-tests. **B-D.** Image visualization by pseudocoloring of baseline and on-treatment FFPE sections of two representative areas in metastatic pancreatic tumor biopsies taken from one Arm A patient who exhibited stable disease. FFPE sections are stained via Multiplex IHC for (**B**) $CD45^+CD4^+$ T helper cells (red arrow), $CD45^+CD8^+$ cytotoxic T cells (blue arrow), (**C**) $CD45^+CD4^+Foxp3^+$ T regulatory cells (blue arrow), (**D**) $CD45^+CSF1R^+CD68^+CD163^+$ M2 macrophages (red arrow), and $CD45^+CSF1R^+CD68^+CD163^-$ M1 macrophages (blue arrow). **E.** Comparative analysis of $CD8^+$ T cell functional status at baseline and on-treatment.

Table 1.

Demographics, disease, and treatment history among participants who received at least one treatment.

Characteristics	All Participants N = 82	Arm A N = 40	Arm B N = 42
Age at randomization (years), Median (1st-3rd Q)	61 (56 to 68)	60 (55 to 65)	62 (58 to 70)
Male, N(%)	49 (60%)	23 (57%)	26 (62%)
Caucasian, N(%)	71 (87%)	35 (88%)	36 (86%)
Months since stage IV diagnosis, Median (1st-3rd Q)	6 (5 to 8)	6 (5 to 8)	7 (5 to 8)
Initial stage, N(%)			
IB-IIB	24 (29%)	12 (30%)	12 (29%)
III	2 (2%)	0 (0%)	2 (5%)
IV	56 (68%)	28 (70%)	28 (67%)
ECOG 0	31 (38%)	12 (30%)	19 (45%)
Histologic grade, N(%)[a]			
Well differentiated/Moderately differentiated	39 (48%)	20 (48%)	19 (45%)
Poorly differentiated	22 (36%)	10 (33%)	12 (39%)
Unknown	21 (26%)	10 (25%)	11 (26%)
Pancreatic tumor location, N(%)			
Head	40 (49%)	18 (45%)	22 (52%)
Body	27 (33%)	11 (28%)	16 (38%)
Tail	22 (27%)	14 (35%)	8 (19%)
Neck	1 (1%)		1 (2%)
Metastatic sites at randomization, N(%)[b]			
Liver	58 (71%)	27 (68%)	31 (74%)
Lung	19 (23%)	10 (25%)	9 (21%)
Lymph nodes	5 (6%)	2 (5%)	3 (7%)
Peritoneum	15 (18%)	11 (28%)	4 (10%)
Other[c]	3 (4%)	2 (5%)	1 (2%)
CA19–9 secretors (elevated either on study or prior to enrollment), N(%)	63 (76.8%)	32 (80%)	31 (73.8%)
CA19–9 at baseline - Normal	11 (17.5%)	5 (15.6%)	6 (19.4%)
CA19–9 at baseline - Elevated, <59xULN	44 (69.8%)	20 (62.5%)	24 (77.4%)
CA19–9 at baseline - Elevated, ≥59xULN	8 (12.7%)	7 (21.9%)	1 (3.2%)
Albumin at randomization, Median (1st-3rd Q)	4 (3.7 to 4.2)	3.9 (3.6 to 4.2)	4 (3.7 to 4.1)
Prior pancreatectomy	22 (27%)	10 (25%)	12 (29%)
Prior radiation therapy	16 (20%)	8 (20%)	8 (19%)
Number of cycles of FFX, Median (1st-3rd Q)	10 (8 to 12)	10 (8 to 12)	10 (8 to 12)

[a]Percent missing is computed out of the total number of participants. Percent within each category is calculated out of the number with available data.

[b]The numbers will total more than 100% since patients could have more than one disease location.

[c]Other includes 1 patient each with the following: chest wall and paraspinal, IVC and right perirenal mass, and bone.

Q = Quartile; N = number; % = percent; kg = kilogram; cm = centimeter; m = meter.